Self-Assembly of Supramolecular Polymers of N-Centered Triarylamine Trisamides in the Light of Circular Dichroism: Reaching Consensus between Electrons and Nuclei

Koenis, M.A.J.; Osypenko, A.; Fuks, G.; Giuseppone, N.; Nicu, V.P.; Visscher, L.; Buma, W.J.

DOI
10.1021/jacs.9b11306

Publication date
2020

Document Version
Final published version

Published in
Journal of the American Chemical Society

JACS JOURNAL OF THE AMERICAN CHEMICAL SOCIETY

Article

Cite This: J. Am. Chem. Soc. 2020, 142, 1020−1028

pubs.acs.org/JACS

Self-Assembly of Supramolecular Polymers of N-Centered Triarylamine Trisamides in the Light of Circular Dichroism: Reaching Consensus between Electrons and Nuclei

Mark A. J. Koenis,[†] Artem Osypenko,[‡] Gad Fuks,[‡] Nicolas Giuseppone,[‡] Valentin P. Nicu,[§] Lucas Visscher,[∥] and Wybren J. Buma*[,†,⊥]

[†]Van 't Hoff Institute for Molecular Sciences, University of Amsterdam, Science Park 904, 1098 XH Amsterdam, The Netherlands

[‡]SAMS Research Group, Institut Charles Sadron, University of Strasbourg, CNRS−23 rue du Loess, BP 84047, 67034 Strasbourg Cedex 2, France

[§]Department of Environmental Science, Physics, Physical Education, and Sport, Lucian Blaga University of Sibiu, loan Ratiu Street, Nr. 7-9, 550012 Sibiu, Romania

[∥]Amsterdam Center for Multiscale Modeling, Section Theoretical Chemistry, Faculty of Sciences, Vrije Universiteit Amsterdam, De Boelelaan 1083, 1081 HV Amsterdam, The Netherlands

[⊥]Institute for Molecules and Materials, FELIX Laboratory, Radboud University, Toernooiveld 7c, 6525 ED Nijmegen, The Netherlands

Supporting Information

ABSTRACT: The self-assembly of chiral supramolecular polymers is an intricate process that spans a wide range of length scales. Circular dichroism techniques are ideal to study this process as they provide information on the molecular scale but are at the same time also sensitive probes of the long-range interactions that control the growth and morphology of these polymers. As yet, Electronic Circular Dichroism that uses electronic transitions as a probe has by far been the method of choice while Vibrational Circular Dichroism, which uses vibrational transitions to probe structure, is much less employed. Here, we report experimental and theoretical studies of the self-assembly of helical supramolecular polymers of (*S*)-triarylamine tris-amides ((*S*)-TATA) in which both techniques are applied in concert. Theoretical studies based on quantum chemical calculations and on simplified models that allow for extrapolation to "infinitely" long polymers provide a solid basis for interpreting results from each of the two techniques that on their own would appear to be contradictory. In the particular case of (*S*)-TATA it is shown that upon equilibration the initially formed fibers undergo a conformational transition that becomes only "visible" by the combination of the two techniques. Our studies thus show that combining electronic and vibrational domains offers a unique and complementary means to probe these polymers, precisely because they are sensitive to different aspects of molecular and polymeric structure.

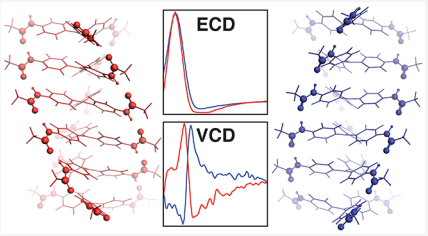

INTRODUCTION

Self-assembly offers an attractive and versatile route toward the rational development of functional materials with targeted properties. At the same time, it is a process that is also of key importance in nature. The process of supramolecular assembly and aggregation is thus attracting major attention from a wide range of scientific disciplines.[1−3] Interests range from the formation of amyloid fibrils[4−6] associated with neurodegenerative diseases like Alzheimer and Parkinson, to material sciences where organic supramolecular polymers show a highly varying range of structural as well as ionic, electronic, and photonic transport properties.[3,7−11] These properties depend strongly on the morphology of the assembly at different scales; from their exact monomeric structure at the nanoscale to the aggregation of their supramolecular complexes at the mesoscale.[12−14] To gain control over such functional properties a fundamental understanding of the supramolecular self-assembly mechanism is essential.

The supramolecular chirality that these polymers often exhibit and that frequently forms the basis for their use in applications offers in this respect an ideal means to study the self-assembly process with chiroptical techniques such as electronic circular dichroism (ECD) and vibrational circular dichroism (VCD) since these techniques are in particular sensitive to the detailed spatial structure of the overall assembly.[2,3,15,16] Although ECD (and to a much lesser extent VCD) is often employed to characterize the stereochemical properties of self-assembled polymers, it is striking to see that the analysis of these spectra so far mainly has been done at a qualitative level. That is, as a general rule the analysis primarily

Received: October 21, 2019
Published: December 23, 2019

DOI: 10.1021/jacs.9b11306
J. Am. Chem. Soc. 2020, 142, 1020−1028

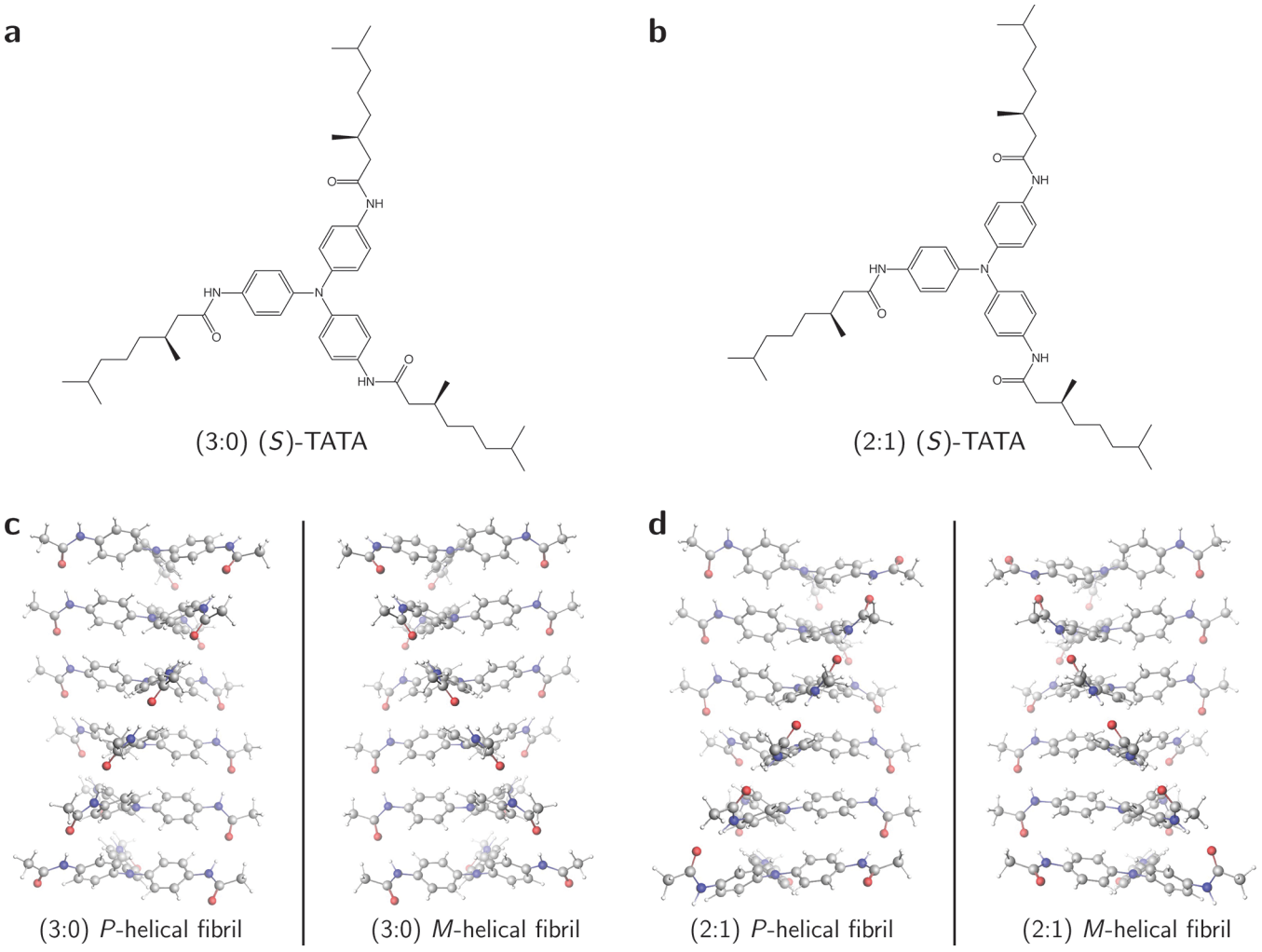

Figure 1. Molecular structure of the (3:0) (a) and (2:1) (b) conformations of (*S*)-triarylamine trisamide ((*S*)-TATA). Schematic representation of helical stacks of the (3:0) (c) and (2:1) (d) conformations of (*S*)-TATA.

focuses on changes in signs of bands under different assembly conditions but does not validate and obtain further insight into the experimental results by quantitative theoretical methods. The present study distinguishes itself in that respect as it aims to obtain a solid support for the interpretation of VCD and ECD spectra by explicit calculations of these spectra for monomers and supramolecular assemblies.

In the present study we focus on the supramolecular polymerization of N-centered C_3-symmetric triarylamine trisamides (TATA, see Figure 1a and b). The stacking of the TATA units is facilitated by $\pi-\pi$ stacking interactions between the phenyl groups as well as by hydrogen bonds between the amide groups of adjacent TATA units. This causes the central nitrogen atoms of the TATA molecule to form a colinear arrangement in helical monocolumnar stacks (i.e., fibrils) with *M* or *P* chirality, the two helicities having identical energies (see Figure 1c and d).[17] However, by introducing a chiral center in all or just a small fraction of the side chains of the TATA core, a preference for either the *M* or *P* helicity is created,[16] ultimately leading to supramolecular aggregates with a single chirality. Such stacks exhibit large CD signals that are critically dependent on the polymerization process and can thus be used to follow the process in detail.

Recently, we reported on studies on the supramolecular polymerization of (*S*)-TATA, and in particular on steering the supramolecular structure and chirality by means of different temperature trajectories.[18] This was done by cooling a hot solution to room temperature with either a fast or a slow rate, and analyzing using a variety of techniques including ECD and VCD. In particular, we established that a sequential supramolecular polymerization mechanism could take place by slow cooling, leading first to *P*-fibrils and then to *M*-superhelices made of these *P*-fibrils (see Pathways I and II in Figure 7). In the present work, we now show that under certain experimental conditions ECD and VCD spectra lead to opposing conclusions on the helicity of the produced assemblies. As yet, ECD and VCD studies are rarely combined.[19] In fact, in practice it is often tacitly assumed that the two techniques depend similarly on the structural parameters of interest, implying that sign inversions in one of the spectra are accompanied by sign inversions in the other. From a theoretical point of view this clearly does not need to be the case, and it is therefore of key interest to study how structural changes in well-defined systems such as the (*S*)-TATA supramolecular assemblies studied here affect each of the two types of spectra. As we will show, a careful analysis of these spectra actually offers a unique possibility to zoom in on different and complementary details of their structure.

Remarkably, we found in the present studies that the VCD spectrum of samples that had been cooled at 0 °C or stored at

DOI: 10.1021/jacs.9b11306
J. Am. Chem. Soc. 2020, 142, 1020−1028

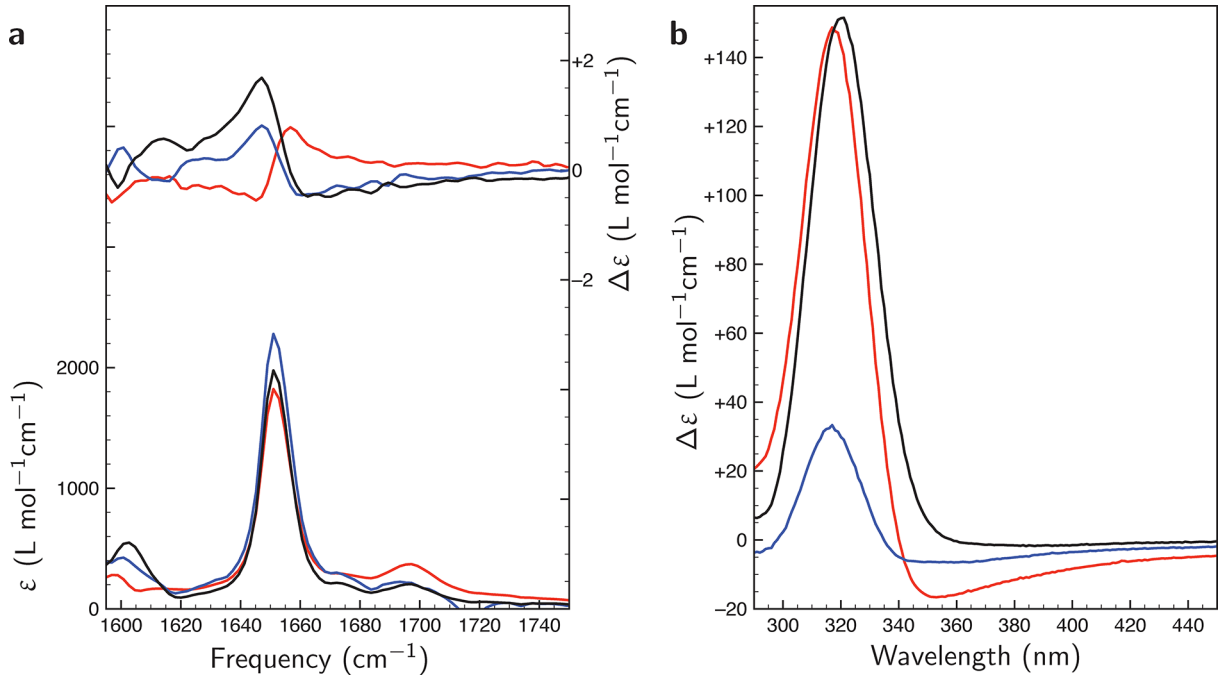

Figure 2. Comparison between the (a) VA (bottom panel), VCD (top panel), and (b) ECD spectra of 1 mM solutions of (*S*)-TATA in toluene-d_8 for different cooling conditions and equilibration times. The blue spectra have been recorded on a fresh sample cooled on ice, and the red spectra on a fresh sample cooled to air, while the black spectra have been measured on a sample that was cooled to air and stored for two months at room temperature.

room temperature for a longer period (on the order of weeks) showed a sign inversion of the amide I bands, indicating a change in helicity. The latter observation is intriguing, in particular in the context of the studies of Meijer et al. on N-centered TATAs with reversed amide moieties.[20] In these studies it was found that two stable self-assembled states of opposite helicity can be formed. At high temperatures, stacks are formed via a nucleation-elongation mechanism of monocolumnar fibrils in which all three amide groups have the same orientation and the hydrogen-bonding dipoles between stacks are aligned parallel, indicated as the (3:0) conformation. Below room temperature, however, a second state is formed in which one of the amide groups of each TATA molecule is rotated -leading to two parallel and one antiparallel dipole indicated as the (2:1) conformation- and which is accompanied by inversion of the fibril helicity. For the N-centered (*S*)-TATAs studied here such a kinetic trapping has not been reported yet, but clearly is of considerable interest.

In order to come to a consistent interpretation of these results, we report here extensive computational studies on the VCD and ECD spectra of (*S*)-TATA monomers and their stacks. We furthermore performed additional VCD and ECD measurements at different concentrations and different cooling conditions. We do such a theoretical study at the ab initio level, but ultimately also compare the results with the results of calculations based on a coupled oscillator model. Such a connection is instructive as it allows one to extend and extrapolate the present results to larger assemblies, but also allows to test the validity of such an approach for other types of assemblies. We will show that the experimental results can be consistently interpreted on the basis of these computational analyses, and that these computational analyses allow us to identify the key elements that determine the appearance of the ECD and VCD spectra of (*S*)-TATA supramolecular polymers. At a more general level, our results pave the way for further detailed studies of supramolecular polymerization processes at large.

EXPERIMENTAL RESULTS

Figure 2 displays Vibrational Absorption (VA), VCD, and ECD spectra recorded for 1 mM solutions of (*S*)-TATA in toluene-d_8 with different equilibration times, using either cooling from hot solutions to room temperature, or from hot solutions to 0 °C (see Supporting Information, SI section S1.1 for further experimental details). The ECD spectra show for all employed conditions basically the same positive/negative bisignated band although the relative intensities of the positive and negative parts depend on the particular conditions under which the spectrum has been recorded. These spectra are in agreement with the spectra reported in our previous studies in which it was concluded that they are associated with an *M*-superhelical arrangement of *P*-helical (*S*)-TATA fibers.[18]

As a result of the high absorbance of the solvent and the very low absorbance of the solute (see SI Figure S4) VCD spectra can only be recorded in the amide I region. In view of the ECD results, one expects that the sign pattern of the bands in these VCD spectra would not depend on the experimental conditions. Interestingly, this is not borne out by the experiments which show that the air-cooled sample exhibits an opposite coupling pattern from the other two samples. Follow-up experiments in which these measurements were repeated and in which measurements were done at different concentrations confirmed these observations, the only possible difference being that for higher concentrations sign inversion appeared to require a longer equilibration time (see SI Figure S5).

Although the ECD and VCD experiments thus consistently showed the same sign patterns, it was at the same time observed that the relative intensities of the bands in the ECD and VCD spectra differed strongly from sample to sample (see Figures 2, S5, and S6). These differences might in part be attributed to the fact that the supramolecular helices form a gel, which could easily lead to inhomogeneities in sample concentration. However, we also observed

DOI: 10.1021/jacs.9b11306
J. Am. Chem. Soc. 2020, 142, 1020−1028

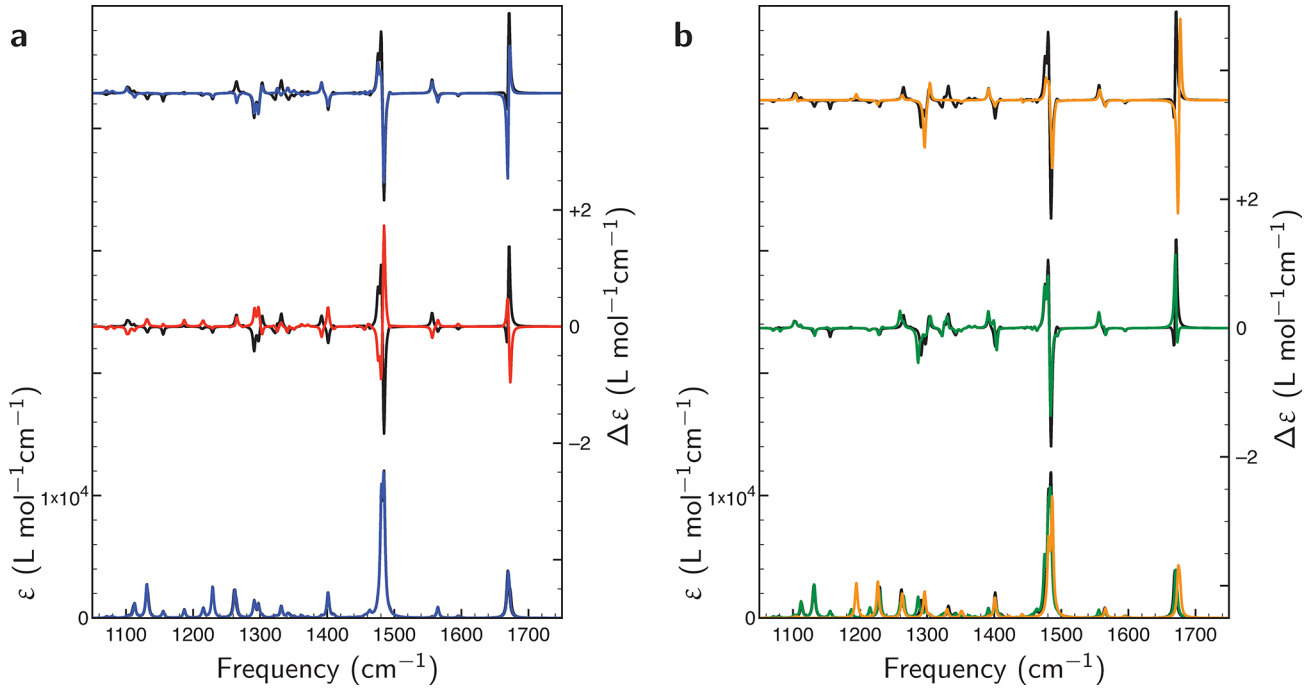

Figure 3. Computed VA (bottom panel) and VCD (middle and upper panel) spectra of monomeric (*S*)- and (*R*)-TATA in which (*S*)-TATA (black) with the three chains oriented along the directions they adopt in *P*-helical stacks of these monomers is always compared with other structures. (a) Comparison for the (3:0) conformation: relative to *M*-oriented (*S*)-TATA (red) and *P*-oriented (*R*)-TATA (blue). (b) Comparison with the *P*-oriented (*S*)-TATA (2:1) conformation (green), and with the *P*-oriented (*S*)-TATA (3:0) conformation (orange) with the chiral carbon chains replaced by a methyl group. Spectra have been convoluted using a full width at half-maximum of 4 cm^{-1} for a better resolution of the individual bands.

variations in the *relative* ratio of the intensities of bands in the IR and VCD spectra, and such variations cannot be explained by a difference in the absolute concentration. Instead, they strongly suggest that the samples contain mixtures of *M*- and *P*-helical stacks, and that the sign pattern is determined by which type of helix is dominantly present. This conclusion finds further support from a recent study by the Meijer group in which a temperature-dependent equilibrium between *M*- and *P*-helical stackings has been described for an (*S*)-TATA system with reversed amides.[20] Such an equilibrium between *M*- and *P*-helical structures might in principle explain the sign change in the VCD spectrum over time since this could then be the result of an initial kinetic trapping of the (3:0) conformation which over time is converted into the more stable (2:1) conformation.

What this mechanism, however, fails to explain are the observed differences between the ECD and VCD spectra, that is, the ECD spectra always show the same signs while the signs in the VCD spectra are dependent on the experimental conditions. Moreover, it is a priori not clear whether the (3:0) and (2:1) products indeed have a different sign in the VCD spectrum (as implicitly assumed above), or that it is the *M*- to *P*-helical reorganization or even a combination of the two that is responsible for the sign change. In fact, one quickly comes to the conclusion that to elucidate the experimental observations a much better understanding is needed of what determines the signs and intensities of the ECD and VCD bands in these supramolecular systems.

THEORETICAL ANALYSIS

In the following we will in first instance discuss results of theoretical calculations on the VCD and ECD spectra of conformations of individual TATA molecules. We will then use these results to determine how stacking of TATA molecules into polymeric chains influences these spectra by performing calculations on various polymeric TATA chains. Finally, we will set up a simplified model based on a coupled oscillator approach and determine to what extent such a model is able to reproduce the relevant aspects of the spectra. Ultimately, we will use this model to explain the different sensitivities of the ECD and VCD spectra to structural parameters.

Coupling in Monomeric (*S*)-TATA. Figure 3a displays computed VA and VCD spectra of (*R*)- and (*S*)-TATA with the three chains oriented along the directions they adopt in *M*- and *P*-helical stacks of these monomers (see SI section S1.2 for theoretical details). For brevity we will refer to these orientations in the following discussion on monomeric TATA as *M*- and *P*-orientations. As expected, the VA spectra are identical for these systems since this technique is not sensitive to the chirality of the molecule. The VCD spectra, however, give rise to a number of—at first sight—surprising observations, the most important one being that (*R*)- and (*S*)-TATA have almost identical VCD spectra. The chirality of the three individual chiral centers thus has very little effect on the signs of the VCD bands. Changing the orientation of the three chains from *M* to *P*, however, gives rise to a near-perfect sign inversion of VCD bands. It is therefore clear that VCD is much more sensitive to the orientation of the chains than to the actual chiral centers in the molecules. Interestingly, there are still some modes that only depend on the molecular chirality, the most clear example being the 3-fold degenerate mode at 1265 cm^{-1}. The reason that this particular mode shows sign inversion on going from (*R*)- to (*S*)-TATA is that it corresponds to a CH bending mode localized on the chiral part of one of the carbon chains making it much more sensitive to the chirality of the carbon chains than to the helicity. Overall, we thus come to the conclusion that VCD is indeed able to distinguish easily between *P*- and *M*-orientations but that it is much harder to distinguish (*R*)- from (*S*)-TATA.

DOI: 10.1021/jacs.9b11306
J. Am. Chem. Soc. 2020, 142, 1020−1028

A further important issue is to which extent the VCD signs are sensitive to the relative orientation of the three amide groups. Figure 3b reports to this purpose VA and VCD spectra calculated for the (3:0) and (2:1) conformations. Apart from some small frequency shifts the VA spectra of both conformations do not display major differences. Also the VCD spectra look very similar except—and this is quite important since this is the only region that is experimentally accessible—for the carbonyl stretch region for which a sign inversion is observed. The calculations show here that for the (3:0) conformation the negative, low-frequency band is associated with a 2-fold degenerate asymmetric stretch mode while the positive, high-frequency band derives from the totally symmetric mode as would be expected from standard coupled-oscillator theory (see SI Figure S7).[21] The (2:1) conformation shows a similar behavior but due to the opposite direction of one of the carbonyl groups all signs are inverted, that is, the low-frequency band associated with the out-of-phase combinations of the carbonyl stretches becomes positive, while the high-frequency band associated with the in-phase combination obtains a negative sign (see SI Figure S7).

Figure 4 displays calculated electronic absorption and ECD spectra of the (3:0) and (2:1) conformations of the TATA

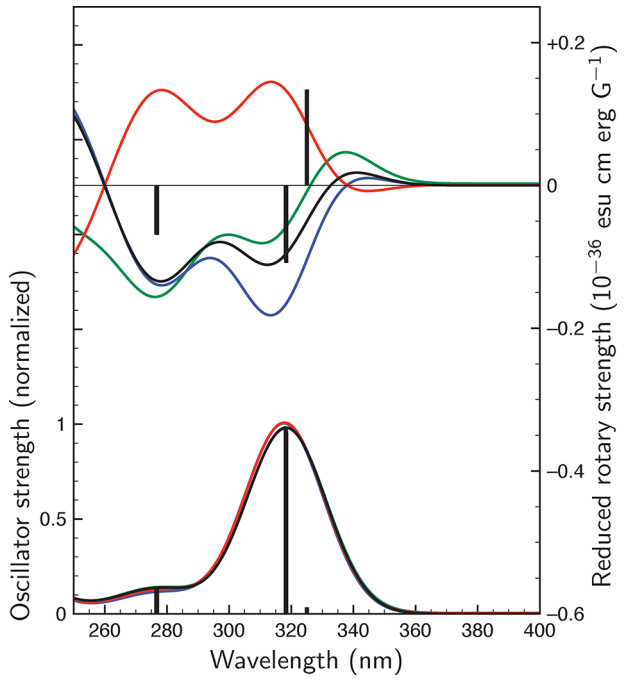

Figure 4. Comparison of computed electronic absorption (bottom panel) and ECD (top panel) spectra of monomeric (*S*)- and (*R*)-TATA. Color coding as in Figure 3. Black, red, and blue traces are associated with the *P*-oriented (*S*)-TATA, *M*-oriented (*S*)-TATA, and *P*-oriented (*R*)-TATA (3:0) conformation while the green trace is associated with the *P*-oriented (*S*)-TATA (2:1) conformation. Theoretical stick spectra have been convoluted using a Gaussian with a full width at half-maximum of 30 nm for comparison with the experimental spectra.

monomer with the three side chains in various orientations. These calculations show that the relevant bands observed in the ECD spectrum derive from $\pi-\pi^*$ transitions of the three substituted-benzene chromophores. Similar to the VCD spectrum we find that coupling between the three chromophores is dominantly responsible for the intensities and signs in the ECD spectrum, and not the absolute configuration of the chiral center. As a result, sign changes only occur when the orientation of the three side chains is changed but not upon inverting the absolute configuration of the three chiral centers. For the further discussion it is important to notice that calculations on a model compound with a single chromophore and the other two arms replaced by methyl groups show that the electronic transition dipole moment to the lowest excited singlet state—which in the TATA monomer is coupled to the analogous transition dipole moments of the other two benzene chromophores—lies in the plane of the phenyl group and is quasi parallel with the direction of the arm (see SI Figure S9). As to be expected, rotation of one of the three side arms to yield the (2:1) conformation does not affect the signs of the CD spectrum as this, for all practical purposes, does not change the direction of the electronic transition dipole moment.

Coupling in Polymeric (*S*)-TATA. Since the chiral carbon chains attached to the TATA-core are quite large, calculations on polymers of the complete molecule are not feasible. We have therefore performed calculations on (*S*)-TATA molecules in which the carbon chains have been replaced by methyl groups. To confirm that this only has a minor influence, VCD spectra have been computed for such methyl-terminated monomeric structures and compared them to the spectra of the original molecule (see Figure 3b). Figure 3b shows indeed that the previously observed coupling behavior -and in particular its dependence on helicity- is preserved and that only some minor-intensity bands associated with the carbon chains are absent in the spectrum of the methyl-terminated compound. We thus conclude that the spectra of these compounds are representative for the spectra of the original TATA molecules.

Figure 5a shows VA and VCD spectra computed for polymeric *P*-helical (*S*)-TATA stacks of different sizes. In going from the monomeric to the polymeric structures several significant changes occur. First, in the polymeric systems hydrogen bonds are formed between the N−H and C═O groups of neighboring (*S*)-TATA molecules. As a result, the intrinsic frequency of the carbonyl stretch mode is red-shifted by about 20 cm^{-1}. The observation that a band remains visible at the non-hydrogen-bonded frequency is due to the fact that the carbonyl group of the last molecule in the stack does not make such a hydrogen bond and its frequency therefore remains unaffected. Second, the (3:0) and (2:1) conformations surprisingly only show opposite signs in the VCD spectrum of the monomeric system. Further insight is provided when the normal modes associated with the intensity-carrying bands are considered in more detail. Inspection of the normal modes (see SI Figures S7 and S8) shows that for stacks of the (3:0) conformation these bands have a similar character as in the monomer. For stacks of the (2:1) conformation, however, the in-phase mode becomes the lowest-frequency band and changes in sign, while the out-of-phase combinations—which are degenerate for the (3:0) conformation—are split into two bands with opposite sign and appear at higher frequencies. Finally, it is important to notice that the calculations find that stacks of the (2:1) conformation have a lower energy than stacks of the (3:0) conformation (see SI Table S1), analogous to what has been found for TATAs with reversed amide groups.[20]

Inspection of the normal modes and their frequencies in the various oligomers also allows us to assess the strengths of the

DOI: 10.1021/jacs.9b11306
J. Am. Chem. Soc. 2020, 142, 1020−1028

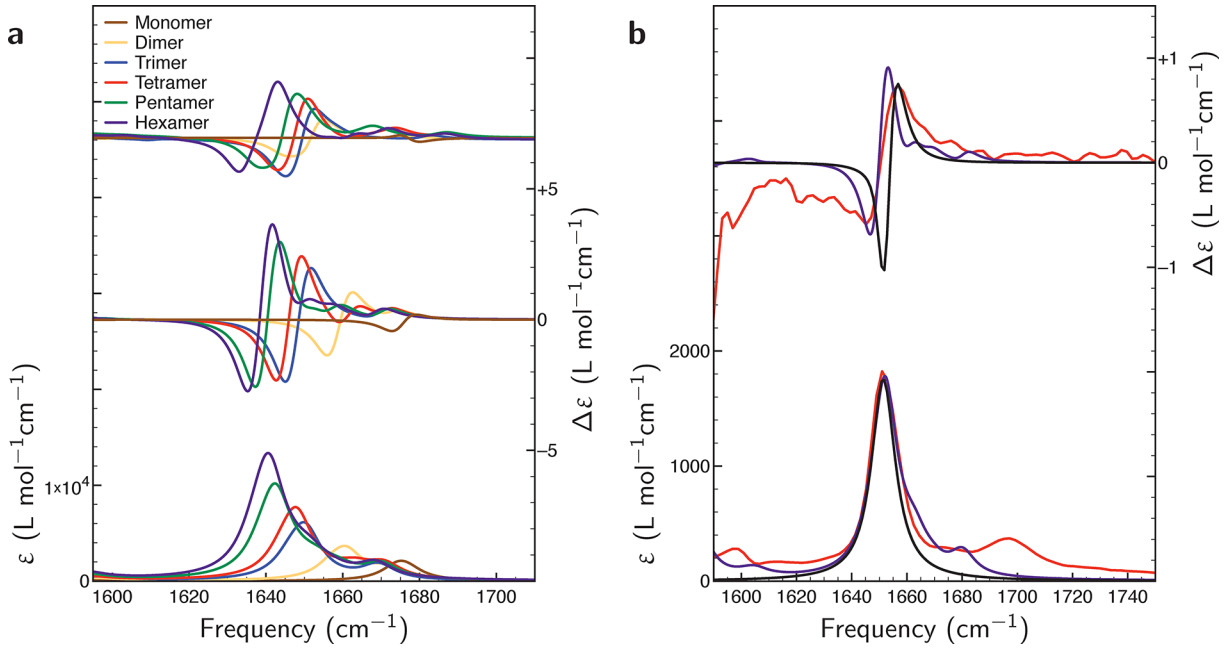

Figure 5. Comparison of calculated VA and VCD spectra of *P*-helical (*S*)-TATA stacks. (a) Comparison between different oligomers ranging from monomer to hexamer. The top and middle panels display VCD spectra of oligomers of (2:1) and (3:0) conformers, respectively, while the bottom panel shows VA spectra of oligomers of the (3:0) conformer. (b) Comparison between VA and VCD spectra calculated for the hexamer (purple) with the experimental spectra of an air-cooled 1 mM (*S*)-TATA solution in toluene-d_8 (red). In order to compare the spectra, intensities in the computed VA and VCD spectra have been reduced by a factor of 7.5 and 4, respectively, while calculated frequencies have been uniformly scaled with a factor of 1.007. The black traces refer to calculations using a simplified coupled oscillator model (see SI Section S2.2.2). In this case intensities in the computed VA and VCD spectra have been reduced by a factor of 28.2 and 4.4, respectively.

intra- and intermolecular couplings. From the nodal patterns of these modes within one TATA molecule and along the stack direction modes can easily be identified that are determined by the intramolecular coupling of the three amide groups within one TATA molecule, and modes whose frequencies are primarily determined by intermolecular coupling along the helical stack direction. From the frequency splittings of these modes we find that the intermolecular couplings are much stronger than the intramolecular couplings. This is in line with expectations based on through-space dipole−dipole interactions since along the helical direction the amide groups are much closer than within one TATA molecule, and with transition dipole moments that are more optimally oriented for dipole−dipole coupling. Apart from these through-space interactions, it should be kept in mind that there are strong hydrogen-bond interactions between the C═O and N−H groups of neighboring TATA molecules within the stacks. As a result, vibrational motion along the carbonyl stretch of a particular TATA molecule in one column of hydrogen-bonded amides will influence the electronic structure of amide groups of neighboring TATA molecules in the other columns. This suggests that the overall coupling between the stacks—and thus the appearance of the VCD spectrum—has contributions from both through-space as well as through-bond interactions.

Comparison of the VA and VCD spectra calculated for the (3:0) hexamer with the experimental spectra (Figure 5b) shows a satisfactory agreement, certainly when bearing in mind that the stacks present in the experimentally observed spectrum are significantly longer than hexamers. Because of this difference in polymer length, the splitting of the band in the VA spectrum is smaller than that observed experimentally, while the widths of the bands in the VCD spectrum are also reduced. It is, however, gratifying to find that the structure observed on the high-frequency side of the VCD band is nicely predicted by the calculations. Calculations on the ECD spectra of TATA-oligomers are out of reach as current-day TD-DFT is not able to provide an adequate description of the electronically excited states of such stacks. However, in this case it is clear that the hydrogen bonds are considerably less important than was observed for the VCD spectra since the pertaining electronic transitions do not involve the amide groups but are localized on the phenyl chromophores. It is therefore reasonable to assume that a satisfactory description of the ECD spectra that is able to elucidate their key features can be obtained using a coupled-oscillator model as will indeed be confirmed in the following.

COUPLED OSCILLATOR MODEL FOR INFINITE (*S*)-TATA STACKS

The quantum chemical calculations have provided detailed insight in key aspects of VCD spectra of monomeric and stacked TATA but as yet it is not clear why the VCD spectrum changes sign over time while the ECD spectrum remains the same. In order to come to a further understanding of the VCD and ECD spectra, and to be able to extrapolate to the "infinitely" long stacks studied experimentally, we have modeled the stacks as a long helix of coupled dipole moments as described by Knoester et al.[22] The absorption and circular dichroism spectrum can then be computed using a Frenkel exciton Hamiltonian with interaction elements between oscillators n and m given by[22,23]

$$J_{nm} = \frac{\vec{\mu}_n \cdot \vec{\mu}_m}{|\vec{r}_{nm}|^3} - 3\frac{(\vec{\mu}_n \cdot \vec{r}_{nm})(\vec{\mu}_m \cdot \vec{r}_{nm})}{|\vec{r}_{nm}|^5} \quad (1)$$

DOI: 10.1021/jacs.9b11306
J. Am. Chem. Soc. 2020, 142, 1020−1028

where $\vec{\mu}$ is the dipole transition moment vector and $\vec{r}_{nm} = \vec{r}_n - \vec{r}_m$ the vector between the positions of the two oscillators. The absorption spectrum of cylindrical systems is then given by the following:[22]

$$A(\omega) = \frac{|\mu|^2}{3}\left[\sum_k \sum_{n,m} c_n^k c_m^k (\cos^2(\beta) + \sin^2(\beta)\cos[(n_2 - m_2)\phi + (n_1 - m_1)\gamma)])\right] F(\omega - E_k) \quad (2)$$

while the corresponding circular dichroism spectrum is obtained as follows:

$$\mathrm{CD}(\omega) = \frac{\pi}{6\lambda}\left[\sum_k \sum_{n,m} c_n^k c_m^k (\vec{r}_{nm} \cdot (\vec{\mu}_n \cdot \vec{\mu}_m))\right] F(\omega - E_k) \quad (3)$$

where c_n^k is the coefficient of oscillator n in eigenvector k, $F(\omega)$ either a Gaussian or Lorentzian broadening function, E_k the k^{th} energy eigenvalue, λ the wavelength of the absorbing light, β the angle between $\vec{\mu}$ and the helical axis, n_1, n_2, m_1, and m_2 the indexes of oscillators n and m along the helical axis (1) and within one TATA molecule (2), ϕ the angle between two oscillators in a TATA molecule and γ the pitch angle (see Figure 6). A full description of the modeling including specifications of the diagonal elements and transition dipole moments for simulation of the VCD and ECD spectra is given in Section S2 of the SI.

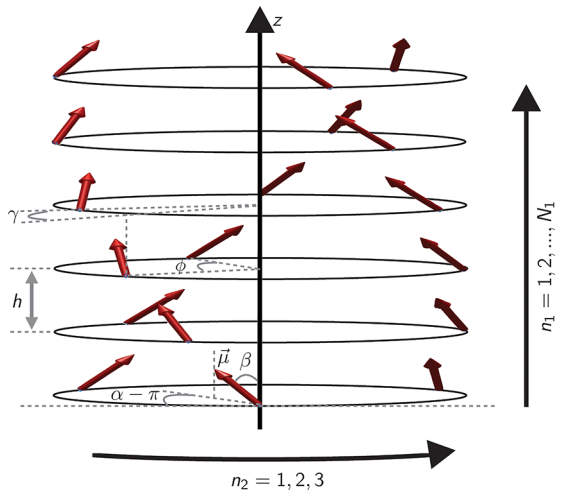

Figure 6. Schematic representation of the interacting dipole moments in the helically stacked structure of (S)-TATA including all the relevant angles and distances for the coupled oscillator model.

The absorption and circular dichroism spectra predicted using the above equations are relatively easy to understand in terms of intensities associated with the purely symmetric and purely degenerate asymmetric combinations of the oscillators, which lead to bisignate bands (see SI Figures S1−S3). For larger stacks, however, interactions between oscillators in different spirals become relevant, and the intensity becomes distributed over more eigenfunctions. Nevertheless, the overall sign pattern of the bisignate band is preserved albeit that the band shape is somewhat distorted as compared to the shorter stacks (see SI Figures S1 and S2). Because of the experimental band broadening these deviations do not show up in the ECD spectrum. For the VCD spectrum, however, the resulting asymmetries in band shape are recognized in the experimental and DFT calculated spectra but not as prominent as that predicted by this coupled oscillator model. We surmise that the underlying reason is the absence of through-bond interactions in the latter model. This is supported by calculations in which we selectively set particular couplings to zero. Models in which the coupling between oscillators that are hydrogen-bonded is set to zero lead to a VCD spectrum that looks almost identical to a pure bisignate band (see Figures 5 and S1). However, when the couplings between amide groups within one TATA molecule are set to zero, the predicted VCD spectrum hardly changes from the spectrum with all couplings taken into account. A more detailed discussion of these results is given in SI Section S2.

The coupled oscillator model enables us to confirm and extend the conclusions drawn from the quantum chemical calculations. For the ECD spectrum of the monomer a spectrum is predicted that is in good agreement with the results of the quantum chemical calculations, while for *P*-helical oriented (*S*)-TATA stacks of the (3:0) conformer a bisignated band is obtained with a negative sign for the low-energy part (SI Figure S3). In the experimental spectrum recorded after fast cooling to room temperature[18] such a negative band is indeed present but it needs to be noticed that the positive part of this bisignated band cannot be observed because of the solvent that is employed. For the VCD spectrum we find similarly that the model predicts signs, splittings, and shifts of the bands that are in good agreement with the results of the quantum chemical calculations (see SI Figure S2). For an increasing number of stacks the coupled oscillator model predicts that the intensity-carrying bands are increasingly red-shifted reproducing the trends observed in the DFT calculations (see Figure 5a). Moreover, when removing the coupling between the hydrogen-bond coupled amide groups the shift also goes to zero indicating that the shift is primarily caused by the interaction between these amide groups.

Importantly, we find that simulations of the VCD spectrum of large *P*-helical stacks (up to 101 stacked (*S*)-TATAs) confirm that the (2:1) conformer indeed only yields opposite signs from the (3:0) conformer for the monomer, and that for higher oligomers bisignate VCD signals with the same signs and about the same frequencies are obtained. As will be argued below, one must therefore conclude that the sign change that is observed in the experimental VCD spectrum when cooling the sample on ice or after equilibration for a long time must be caused by a change in the helicity of the polymers, and that this change in helicity is induced by a transition from the (3:0) conformation—for which the *P*-helix is energetically the most stable form—to the (2:1) conformation for which the *M*-helix has the lowest energy.

In the *M*-superhelical complexes the coupled dipoles are far apart from each other due to the extended carbon chains in the arms. Because of the cubic distance dependence of the coupling strength and the orders of magnitude difference in electronic and vibrational dipole strengths (eq 1), coupling of the vibrational dipoles in different fibrils is then negligible while coupling between the electronic dipoles still persists. As a consequence, the observed VCD signal would only be determined by the coupling within the fibrils while the ECD signal would probe the helicity of the superhelices. In such a picture we can now come to a consistent interpretation of all observations. Upon cooling a solution of (*S*)-TATA molecules

DOI: 10.1021/jacs.9b11306
J. Am. Chem. Soc. 2020, 142, 1020−1028

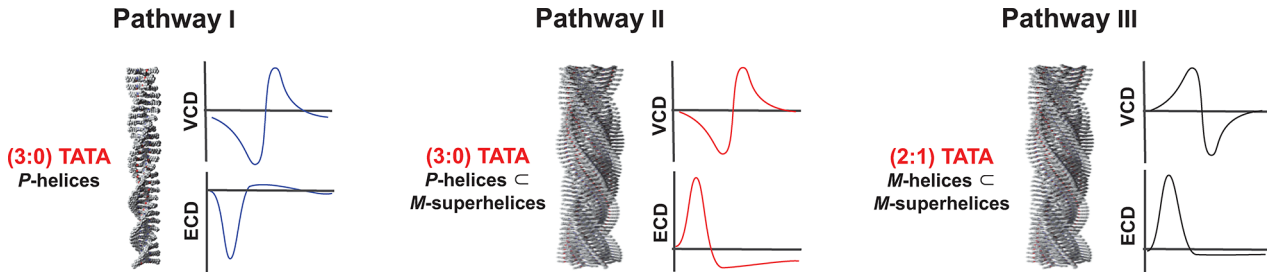

Figure 7. Supramolecular polymers formed by self-assembly of *S*-TATA molecules and their dependence on cooling rate and time scale, together with the ECD and VCD spectra associated with each of these polymers. Pathway I leading to *P*-helical fibers of (3:0) conformers occurs upon fast cooling of a hot solution to room temperature (10 K/min). Pathway II occurs upon slow cooling of a hot solution to room temperature (1 K/min) and leads to the formation of *M*-superhelical fibers of (3:0) *P*-helical fibers. Pathway III resulting in *M*-superhelical fibers of (2:1) *M*-helical fibers is observed when cooling occurs to 0 °C and/or when aging takes place at room temperature over a long period of time (several weeks).

to room temperature, (3:0) *P*-helical fibrils are initially formed as a kinetic product. If the concentration is high enough, and depending on the cooling speed, then *M*-helical superhelices are formed.[18] Because of the difference in coupling strengths such a formation of superhelices does not affect the sign in the VCD spectrum but changes the sign in the ECD spectrum. When these helices are cooled to 0 °C, however, the (3:0) *P*-fibrils are converted into a form in which the helicity of the *P*-fibril is changed while the helicity of the superhelix remains unaffected. Since our quantum chemical calculations predict that polymers of the (2:1) conformation are energetically more stable than polymers of the (3:0) conformation, we conclude that upon cooling to 0 °C or after very long time of equilibration at room temperature (*S*)-TATA molecules undergo a conversion from the (3:0) to the (2:1) conformation and that this is accompanied by a change in helicity of the fibrils but not of the *M*-superhelical structures. These results thus confirm and complement both studies reported in refs 18 and 20.

Although less important for the problem at hand, it is interesting to notice that the coupled oscillator model indicates that the ECD spectra can be expected to be considerably more sensitive to structural inhomogeneities than the VCD spectra. As can be seen from eqs 1 and 3 the sign of the CD signals depends strongly on the orientation of the dipole transition moment with respect to the helical axis. In particular, one notices that the CD signal changes sign when angles α and β (see Figure 6) become larger than 90°. Figure S9 shows that the electronic transition dipole moments lie almost parallel to the three arms of the (*S*)-TATA molecule and thus perpendicular to the helical axis. A small change in the direction of the transition dipole moment would thus already suffice to cause a sign change. The vibrational transition dipole moments, on the other hand, have quite a different direction, making their couplings less susceptible to small changes in the structure.

CONCLUSIONS

In this work an in-depth theoretical analysis has been performed to understand the -at first sight- conflicting behavior of ECD and VCD spectra measured for helical supramolecular polymers of (*S*)-TATA. Quantum chemical studies have revealed that for both ECD and VCD the signals are largely independent of the chirality of the side-chains and are primarily determined by the helical chirality of the supramolecular complex. For monomeric systems the bisignate carbonyl stretch band in the VCD spectrum has been found to change sign upon going from the (3:0) to the (2:1) conformation. In polymeric systems, however, coupling between the different stacks leads to VCD spectra with the same sign pattern for the (3:0) and (2:1) conformations. Quantum chemical calculations of the ECD spectra of polymers are far more difficult, but here one can reasonably expect similar spectra for the two conformations because the electronic transitions are not influenced by a conformational change of one of the amide groups. The calculations thus indicate that only the helicity of the supramolecular assemblies determines the signs of the observed ECD and VCD signals.

Calculations based on a coupled oscillator model lead to spectra that are in good agreement with the quantum chemically predicted spectra, and allow one to extrapolate these results to larger stacks. Aided by such calculations it has been concluded that the sign changes observed in the VCD spectrum when cooling the sample below room temperature and when equilibrating samples for extended periods of time reflect the pathway complexity in the supramolecular assembly process of (*S*)-TATA. Upon cooling multiple products can be formed of which the *P*-helical fibers of the (3:0) conformers are initially favored as the kinetic product. Depending on concentration and cooling conditions these *P*-fibrils coagulate or form *M*-helical superhelices, although it is noticed that the ECD spectra reported in our previous studies indicate that not one single product is initially present.[18] However, thermodynamically fibrils of the (2:1) conformation are more stable, and such fibrils have *M*-helicity. As the VCD spectrum is primarily sensitive to the helicity of these fibrils, while the ECD spectrum reflects the helicity of the overall assembly of fibrils, the VCD spectrum changes over time, while the ECD spectrum is not affected. The combination of the two techniques thus allows for probing chirality at different length scales, similar to studies that try to distinguish "local" from "global" chirality using Raman Optical Activity.[24]

The present studies imply that the VCD spectra presented in Figure 4c of ref 18 should be reinterpreted. The blue spectrum was obtained by cooling the solution to air in The Netherlands just prior to the measurement, which is similar to fast cooling at a rate of 10 °C and leading to *P*-fibrils. The red spectrum, however, was recorded for a solution that had been cooled slowly in Strasbourg and sent to The Netherlands for VCD measurements. Since the CD signal was stable over a very long period of time, the ± bisignate band in the VCD spectrum was at that time attributed to the *M*-superhelix. The present studies show, however, that it should be interpreted as resulting from a molecular inversion of chirality which transforms the *P*-fibrils

DOI: 10.1021/jacs.9b11306
J. Am. Chem. Soc. 2020, 142, 1020−1028

within *M*-superhelices into *M*-fibrils. Such an inversion can easily have occurred during transport of the sample during which it was submitted to low temperatures and to vibrations. Nevertheless, the overall mechanism proposed in Figure 6 of ref 18 remains undiminished valid, and is reinforced by the present study, noticing, however, that a new pathway can take place when cooling the system to 0 °C (see Figure 7).

More generally, our studies have shown that VCD and ECD are in many respects complementary techniques and sensitive to different aspects of structure and morphology. They have also shown that the field has now reached a stage at which quantum chemical calculations can confidently be employed to make predictions on these spectra. It is the combination of both of these techniques and of both theory and experiment that has paved the way for a detailed elucidation of the supramolecular assembly of TATAs in particular, although it is at the same time clear that similar analyses would be quite useful for the study of many other supramolecular assembly processes.

■ ASSOCIATED CONTENT

Supporting Information

The Supporting Information is available free of charge at https://pubs.acs.org/doi/10.1021/jacs.9b11306.

Experimental and computational methods and detailed analysis of computing absorption and circular dichroism spectra on infinity long helical structures and additional figures.(PDF)

■ AUTHOR INFORMATION

Corresponding Author

*w.j.buma@uva.nl

ORCID

Nicolas Giuseppone: 0000-0003-4093-3000

Lucas Visscher: 0000-0002-7748-6243

Wybren J. Buma: 0000-0002-1265-8016

Notes

The authors declare no competing financial interest.

■ ACKNOWLEDGMENTS

M.A.J.K., L.V., and W.J.B. acknowledge financial support from NWO in the framework of the Fund New Chemical Innovations (NWO Project Nr. 731.014.209). V.P.N. acknowledges funding from UEFISCDI (PN-III-P1-1.1-TE-2016-1049, contract nr. 46/2018). N.G. thanks the financial support from icFRC and LabEx CSC. This work was also supported by funds from the ITN READ (Fellowship to A.O.) We are particularly grateful to Prof. Larry Nafie (Syracuse University) for enlightening discussions on fibrils. We furthermore acknowledge useful discussions with Dr. Stan van Gisbergen from SCM.

■ REFERENCES

(1) De Greef, T. F. A.; Smulders, M. M. J.; Wolffs, M.; Schenning, A. P. H. J.; Sijbesma, R. P.; Meijer, E. W. Supramolecular Polymerization. *Chem. Rev.* **2009**, *109*, 5687−5754.

(2) Dzwolak, W. Chirality and Chiroptical Properties of Amyloid Fibrils. *Chirality* **2014**, *26*, 580−587.

(3) Moulin, E.; Armao, J. J.; Giuseppone, N. Triarylamine-Based Supramolecular Polymers: Structures, Dynamics, and Functions. *Acc. Chem. Res.* **2019**, *52*, 975−983.

(4) Dobson, C. M. Protein Misfolding, Evolution and Disease. *Trends Biochem. Sci.* **1999**, *24*, 329−332.

(5) Dobson, C. M. Protein Folding and Misfolding. *Nature* **2003**, *426*, 884−890.

(6) Chiti, F.; Dobson, C. M. Protein Misfolding, Functional Amyloid, and Human Disease. *Annu. Rev. Biochem.* **2006**, *75*, 333−366.

(7) Shirota, Y. Photo- and Electroactive Amorphous Molecular Materials-Molecular Design, Syntheses, Reactions, Properties, and Applications. *J. Mater. Chem.* **2005**, *15*, 75−93.

(8) Hamley, I. Peptide Fibrillization. *Angew. Chem., Int. Ed.* **2007**, *46*, 8128−8147.

(9) Faramarzi, V.; Niess, F.; Moulin, E.; Maaloum, M.; Dayen, J. F.; Beaufrand, J. B.; Zanettini, S.; Doudin, B.; Giuseppone, N. Light-Triggered Self-Construction of Supramolecular Organic Nanowires as Metallic Interconnects. *Nat. Chem.* **2012**, *4*, 485.

(10) Akande, A.; Bhattacharya, S.; Cathcart, T.; Sanvito, S. First Principles Study of the Structural, Electronic, and Transport Properties of Triarylamine-Based Nanowires. *J. Chem. Phys.* **2014**, *140*, 074301.

(11) Wang, J.; Liu, K.; Ma, L.; Zhan, X. Triarylamine: Versatile Platform for Organic, Dye-Sensitized, and Perovskite Solar Cells. *Chem. Rev.* **2016**, *116*, 14675−14725.

(12) González-Rodríguez, D.; Schenning, A. P. H. J. Hydrogen-bonded Supramolecular π-Functional Materials. *Chem. Mater.* **2011**, *23*, 310−325.

(13) Babu, S. S.; Praveen, V. K.; Ajayaghosh, A. Functional π-Gelators and Their Applications. *Chem. Rev.* **2014**, *114*, 1973−2129.

(14) Stupp, S. I.; Palmer, L. C. Supramolecular Chemistry and Self-Assembly in Organic Materials Design. *Chem. Mater.* **2014**, *26*, 507−518.

(15) Sato, H.; Yajima, T.; Yamagishi, A. Chiroptical Studies on Supramolecular Chirality of Molecular Aggregates. *Chirality* **2015**, *27*, 659−666.

(16) Kim, T.; Mori, T.; Aida, T.; Miyajima, D. Dynamic Propeller Conformation for the Unprecedentedly High Degree of Chiral Amplification of Supramolecular Helices. *Chem. Sci.* **2016**, *7*, 6689−6694.

(17) Armao, J. J.; Maaloum, M.; Ellis, T.; Fuks, G.; Rawiso, M.; Moulin, E.; Giuseppone, N. Healable Supramolecular Polymers as Organic Metals. *J. Am. Chem. Soc.* **2014**, *136*, 11382−11388.

(18) Osypenko, A.; Moulin, E.; Gavat, O.; Fuks, G.; Maaloum, M.; Koenis, M. A. J.; Buma, W. J.; Giuseppone, N. Temperature Controlled Hierarchical Supramolecular Polymerization of Chiral Triarylamines. *Chem. - Eur. J.* **2019**, *25*, 13008−13016.

(19) Nicu, V. P.; Mandi, A.; Kurtan, T.; Polavarapu, P. L. On the Complementarity of ECD and VCD Techniques. *Chirality* **2014**, *26*, 525−531.

(20) Adelizzi, B.; Filot, I. A. W.; Palmans, A. R. A.; Meijer, E. W. Unravelling the Pathway Complexity in Conformationally Flexible N-Centered Triarylamine Trisamides. *Chem. - Eur. J.* **2017**, *23*, 6103−6110.

(21) Higgs, P. W. The Vibration Spectra of Helical Molecules: Infra-Red and Raman Selection Rules, Intensities and Approximate Frequencies. *Proc. R. Soc. London, Ser. A* **1953**, *220*, 472−485.

(22) Didraga, C.; Klugkist, J. A.; Knoester, J. Optical Properties of Helical Cylindrical Molecular Aggregates: The Homogeneous Limit. *J. Phys. Chem. B* **2002**, *106*, 11474−11486.

(23) Tinoco, I. The Exciton Contribution to the Optical Rotation of Polymers. *Radiat. Res.* **1963**, *20*, 133−139.

(24) Herrmann, C.; Ruud, K.; Reiher, M. Can Raman optical activity separate axial from local chirality? A theoretical study of helical decaalanine. *ChemPhysChem* **2006**, *7*, 2189−2196.

DOI: 10.1021/jacs.9b11306
J. Am. Chem. Soc. 2020, 142, 1020−1028